



## Late Cretaceous to Early Tertiary transtension and strain partitioning in the Chugach accretionary complex, SE Alaska

J. STEVEN DAVIS and SARAH M. ROESKE

Department of Geology, University of California, One Shields Ave., Davis, CA 95616, U.S.A.

and

SUE M. KARL

U.S. Geological Survey, 4200 University Drive, Anchorage, AK 99508, U.S.A.

(Received 24 February 1997; accepted in revised form 19 December 1997)

**Abstract**—Shear zones in the Late Cretaceous Sitka Graywacke of the Chugach accretionary complex in southeast Alaska record constrictional finite strains, with maximum principal stretches plunging shallowly sub-parallel to strike of the shear zones. Macrostructural analysis indicates the finite strain formed during one deformation event. Microstructural analysis of the shear zones shows that this deformation is ductile, promoted mostly through deformation of low-strength lithic clasts and pressure solution. Kinematic indicators from some of the shear zones indicate dominantly dextral motion. Although multiple scenarios can explain constrictional finite strains in a shear zone, these dextral strike-slip shear zones must have experienced a component of extension across them in order to generate constrictional finite strains. Therefore, the shear zones are dextral transtensional shear zones, an uncommon tectonic regime in an accretionary complex.

The transtensional shear zones reflect strike-slip motion related to partitioning of Late Cretaceous to Early Tertiary right-oblique convergence between North America and the Farallon plate. The extensional component that was superposed on the strike-slip shear zones to generate transtension resulted from contemporaneous collapse of the forearc following thickening related to underplating. © 1998 Elsevier Science Ltd. All rights reserved

### INTRODUCTION

Fitch (1972) originally proposed that plate motion during oblique subduction is partitioned into a component of motion normal to the trench/arc and a component parallel to the arc. Fitch's proposal was based on earthquake first-motion solutions from the western Java Trench and Sumatran Arc that yielded thrust solutions near the trench, and strike-slip solutions in the arc. Subsequent studies (e.g. Jarrard, 1986) used a variety of geophysical evidence to show that strain partitioning commonly occurs at modern obliquely convergent margins. Recently, some authors (e.g. McCaffrey, 1991) have shown that strain partitioning in modern forearcs can be distributed across the forearc region. McCaffrey (1991) used geophysical evidence to suggest that the Sumatra forearc is extending parallel to the trench, thus implying the existence of either normal or strike-slip fault complexes within the forearc that allow the forearc to extend.

Although strain partitioning during oblique convergence is common in the present, examples of partitioning of the plate motions are difficult to document in ancient arc-forearc systems. Studies that document strain partitioning in ancient subduction zone settings usually rely on analyses of brittle faults which show that the trench-parallel component of oblique plate convergence is distributed across the forearc region, in

some cases resulting in trench-parallel stretching of the forearc. In general, the analyzed faults have strike-slip kinematics and trench-parallel strikes like those of the Neogene-Quaternary Hikurangi Margin, New Zealand (Cashman *et al.*, 1992; Kelsey *et al.*, 1995) and the Paleogene-Neogene terrane bounding faults of the Philippines (Karig *et al.*, 1986). In NW Sumatra, strike-slip faults splay off a major trench-parallel strike-slip fault in the volcanic arc and cut obliquely across the forearc to terminate in the trench (Karig *et al.*, 1980). Motion on the splays results in trench-parallel northward stretching of the forearc (McCaffrey, 1991).

Well-documented cases of ancient strain partitioning in accretionary complexes recorded by ductile structures are rare. Avé Lallemant and Guth (1990) analyzed ductile deformation in the mid- to Late-Cretaceous forearc complex of northeastern Venezuela and concluded that exhumation of eclogites and blueschists in the forearc resulted from arc-parallel stretching and thinning of the forearc during oblique convergence. Toriumi and Noda (1986) used analyses of three-dimensional strain in plastically deformed cherts in the Cretaceous Sambagawa Belt to infer the presence of a deep oblique strike-slip shear zone between the accretionary complex and the overriding continental slab, thus implying strain partitioning of the plate convergence.

In all of the studies cited above, the principal result of oblique plate motion partitioning is either along-strike transport of the forearc, or trench-parallel stretching of the forearc. However, there is no reason why forearc extension normal to the trench could not occur coevally with strike-slip plate motion partitioning within the forearc, as is documented for the Hikurangi Margin (Walcott, 1987). Forearc extension normal to the trench can result from a number of mechanisms, but is generally thought to be a response to a change in parameters that govern the maintenance of the critical wedge taper (e.g. Davis *et al.*, 1983). Our study concentrates on deformation of the Late Cretaceous accretionary complex of southeastern Alaska, where existing models show right-oblique convergence between the subducting Farallon plate and the overriding North America plate in the Late Cretaceous (Engebretson *et al.*, 1985). We use field observations from the Cretaceous Sitka Graywacke on Baranof Island (Figs 1 & 2) and three-dimensional finite strain analyses of macroscopically ductile dextral shear zones to show that strain partitioning was active in the forearc during the Late Cretaceous–Early Cenozoic oblique convergence between North America and the Farallon plate. The finite strains in the ductile shear zones are dominantly constrictional, thus implying trench-normal extension and transtensional displacement across the shear zones.

## REGIONAL GEOLOGY

The Sitka Graywacke is part of the Chugach accretionary complex which extends along the entire margin of southern and southeastern Alaska (Plafker *et al.*, 1994). The Chugach accretionary complex records episodic accretion along a subduction margin from the latest Triassic through to the Eocene. In southeast Alaska the crystalline rocks inboard of the Chugach accretionary complex are Wrangellia, part of the Insular superterrane, which contains Paleozoic and Mesozoic island arcs. Final closure of basins between the Insular superterrane and more inboard terranes occurred by the middle Cretaceous (Berg *et al.*, 1972; Monger *et al.*, 1982; Rubin *et al.*, 1990). Although controversy exists concerning the amount of transform displacement of the Insular superterrane following the closure (see Wynne *et al.*, 1995, 1996; Monger and Price, 1996), there is general agreement that, from the Late Cretaceous through to the middle Eocene, convergence between the Pacific plate and the North American plate was accommodated along the western margin of the Insular superterrane (Monger *et al.*, 1994; Cowan, 1994). Thus the Late Cretaceous–Eocene part of the Chugach accretionary complex formed at the subduction zone for the North American plate.

The Chugach accretionary complex in the study area on western Baranof Island consists of a *mélange* facies,

the Khaz *Mélange* of the Kelp Bay Group, to the east and a clastic facies, the Sitka Graywacke, to the west (Fig. 2). The Khaz *Mélange* is pre-Late Cretaceous and consists of metachert, metabasalt, metatuff, and metagraywacke in an argillite matrix (Johnson and Karl, 1985). The Sitka Graywacke is the most oceanward exposure of the Chugach accretionary complex and consists of a thick clastic unit, dominantly metagraywacke and meta-argillite. Decker *et al.* (1979) describe the Sitka Graywacke on western Chichagof and Baranof Islands as primarily a mid-fan facies turbidite assemblage consisting of medium- to coarse-grained sandstone intercalated with rare mudstone. Inner-fan facies assemblages are less common but predominate in our study area (Decker *et al.*, 1979). Thus, the study area on western Baranof Island consists of massive coarse-grained to pebbly sandstone and minor granule to cobble conglomerate. Regional metamorphism of the Sitka Graywacke is zeolite, prehnite-pumpellyite, and locally low greenschist facies (Decker *et al.*, 1979).

The depositional and accretionary age of the Sitka Graywacke is not precisely known. Fossil collections from rocks inferred to be the Sitka Graywacke have been identified as Early Cretaceous (Reed and Coats, 1941). A minimum age of accretion for the Sitka Graywacke is 50 Ma, based on U–Pb and K–Ar dates of a pluton that intrudes it (Bradley *et al.*, 1993). The depositional age of the Sitka Graywacke is most likely post-Early Cretaceous. Inboard of the Sitka Graywacke, cherts in the Kelp Bay Group contain Early Cretaceous radiolaria (Johnson and Karl, 1985), indicating their incorporation in the *mélange* occurred after this time. Although post-accretionary dextral strike-slip faulting has locally disrupted the original margin (Karl *et al.*, 1990; Haeussler *et al.*, 1994) (see below), regional geological relations indicate that the *mélange* facies accreted to the margin prior to the clastic facies. This interpretation of a Late Cretaceous age for the Sitka Graywacke is consistent with its continuity along strike with other clastic assemblages of the Chugach terrane (Plafker *et al.*, 1977). Although fossils from the clastic assemblages along strike to the Sitka Graywacke are rare, they are consistently Late Cretaceous in age (Early Maastrichtian and Late Campanian) (Plafker *et al.*, 1994).

### *Regional structure*

The structural grain of Chichagof and Baranof Islands is predominantly northwest, parallel to the boundary between the accretionary complex and the crystalline rocks to the east. Bedding, cleavage, and axial surfaces of megascopic folds are commonly parallel and dip steeply SW–NE. Penetrative, regional deformation in both the *mélange* and clastic assemblages are synmetamorphic and assumed to be associated with accretion. The regional fabric in the

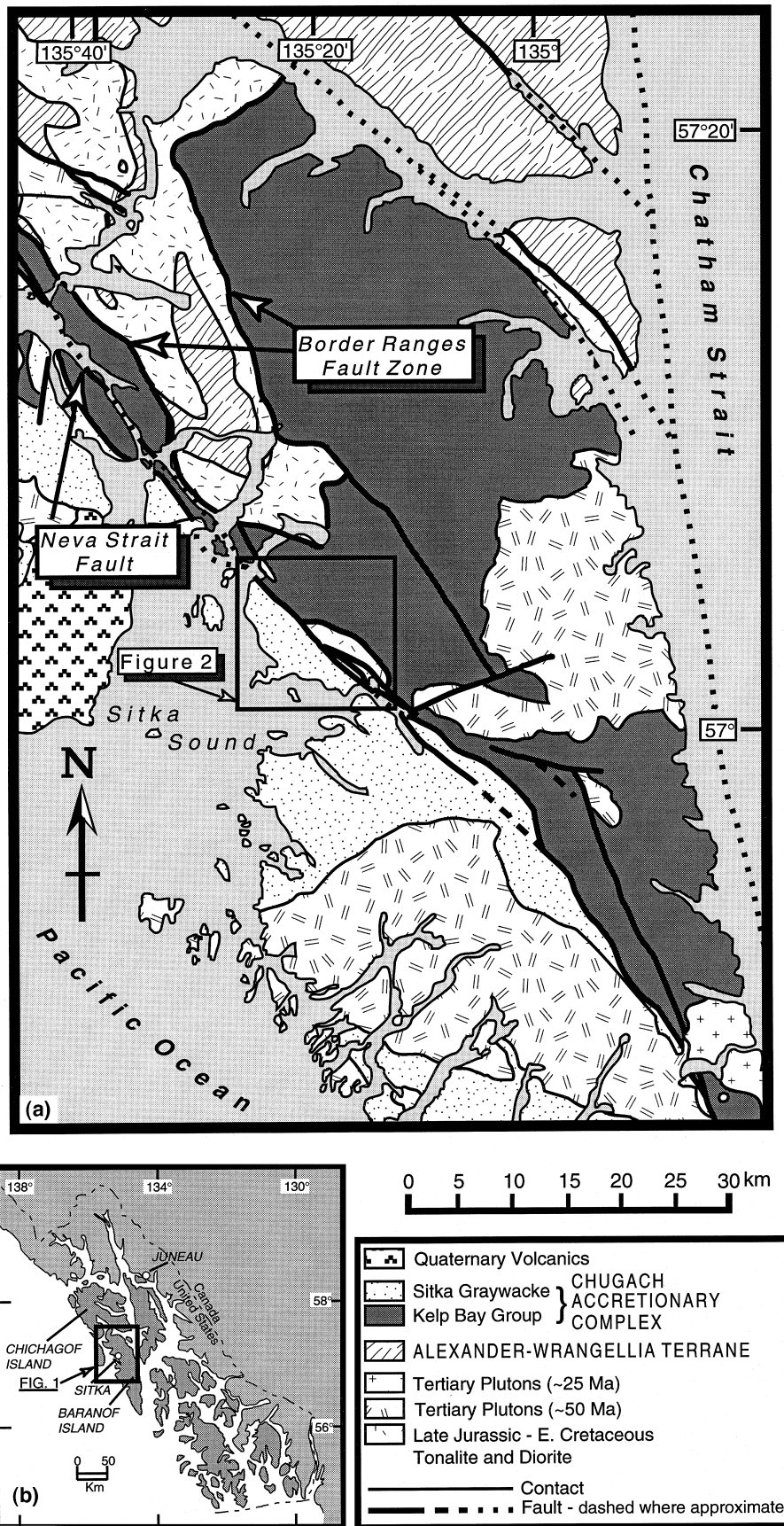


Fig. 1. Generalized geology of northern Baranof Island and southernmost Chichagof Island. Note location of the Chugach and Alexander-Wrangellia Terranes.

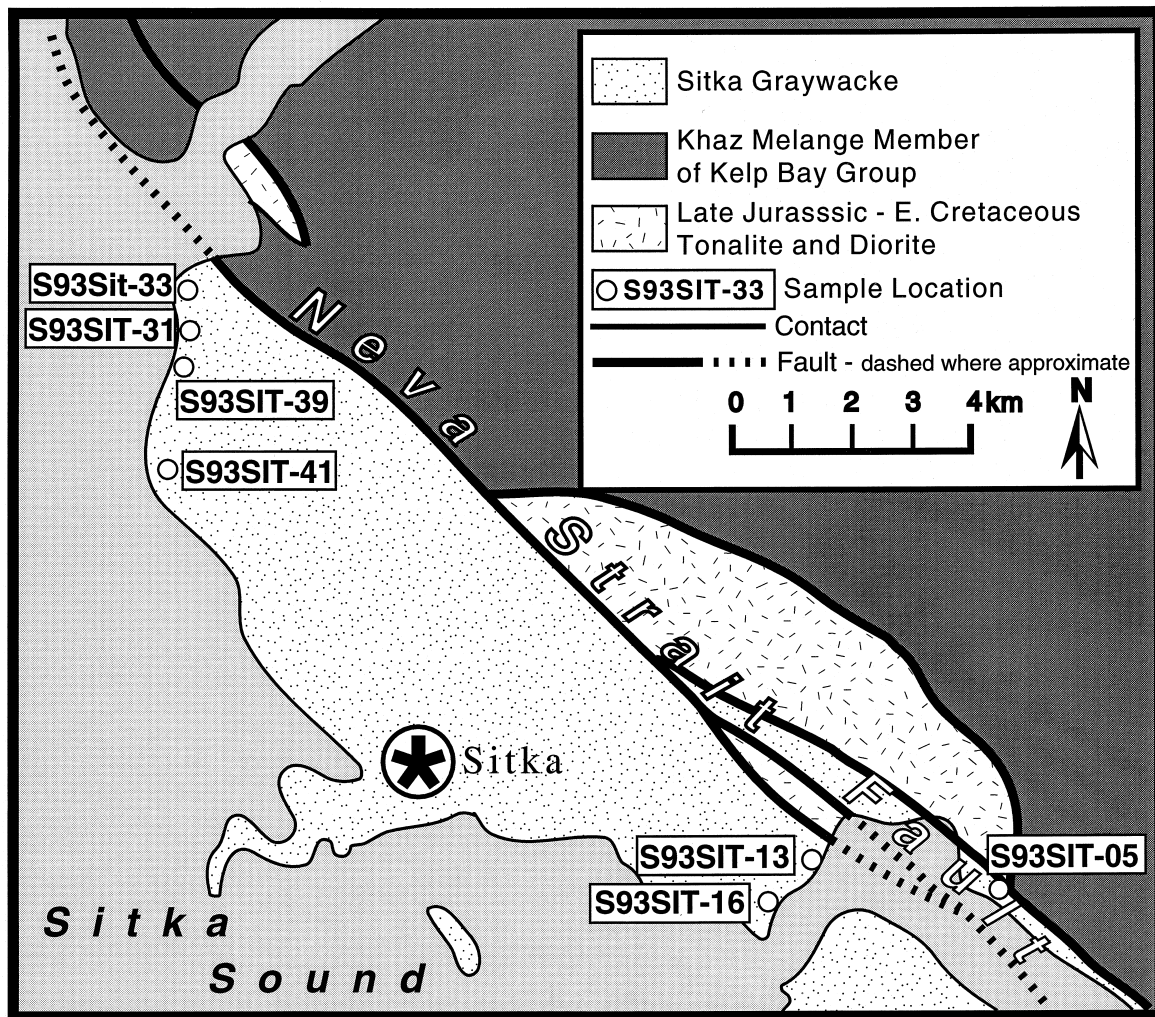


Fig. 2. Generalized geology of the field area and locations of samples used for strain analysis in this study.

Khaz M $\acute{e}$ lange is a scaly cleavage which cross-cuts lithologic layering. Locally a planar cleavage is the dominant fabric in the m $\acute{e}$ lange, particularly on the western margin of the Khaz M $\acute{e}$ lange where a planar cleavage clearly overprints the scaly cleavage. On western Chichagof Island, where the Sitka Graywacke is typically a medium-bedded sandstone–mudstone unit, the rocks are a ‘broken formation’ characterized by pervasive deformation and rotated strata (Decker *et al.*, 1979). The massive-textured thick-bedded sections of the Sitka Graywacke in the study area appear less deformed than the medium-bedded sections to the north, with the exception of the high-strain zone that is the subject of this study.

High-angle brittle faults extensively cross-cut all of the units on Chichagof and Baranof Island and have disrupted the original accretionary boundary to the extent that crystalline rocks of Wrangellia are locally outboard of the m $\acute{e}$ lange assemblage of the Chugach accretionary complex (Karl *et al.*, 1990). The faults have a wide range of orientations and sense of offset

but overall they are characterized by right-lateral strike-slip to oblique slip (Haeussler *et al.*, 1994). Many of the brittle faults reactivate earlier-formed faults; thus major zones of brittle deformation are observed along the boundary between the crystalline rocks and the Chugach accretionary complex (the Border Ranges fault system), and along the boundary between the m $\acute{e}$ lange assemblage and clastic assemblage within the Chugach accretionary complex (the Neva Strait Fault, which reactivates part of the ductile high strain zone of this study). The Border Ranges fault system is interpreted as a thrust fault (Plafker *et al.*, 1976; Decker and Johnson, 1981), but this early dip-slip history is only locally preserved in southeast Alaska. The main dextral brittle fault system on western Baranof is called the Neva Strait–Slocum Arm fault system (Loney *et al.*, 1975). The age of displacement on this fault system is middle Cenozoic, as it cross-cuts a 50 Ma pluton and is intruded by 25 Ma plutons (Loney *et al.*, 1975; Bradley *et al.*, 1993).

## DEFORMATION OF THE SITKA GRAYWACKE

### *Macroscopic deformation*

In the outcrops and samples examined and utilized for this study, the Sitka Graywacke contains few mesoscale structures typical of soft sediment deformation (e.g. layer-parallel pinch and swell, slump folds, load casts), liquefaction (e.g. clastic dikes and pipes), fluid escape (e.g. elutriation horizons), and hydrofracturing (e.g. vein-filled fractures). The rarity of these structures indicates that little soft sediment deformation occurred and that most of the intraformational fluid was expelled by general, pervasive flow under conditions of relatively low confining pressures (cf. Cloos and Shreve, 1988). We infer from the almost total absence of soft sediment deformation structures, as well as the presence of stretched conglomerate clasts (see below), that the Sitka Graywacke was deformed in a lithified state. Therefore, the finite strains recorded in the penetrative deformation zones of the Sitka Graywacke should reflect the tectonic setting(s) in which they formed.

Most of the bedding of the Sitka Graywacke in the study area is massive, strikes northwest and dips shallowly to steeply northeast and southwest (Fig. 3c). However, in some zones the graywacke shows moderately to well developed macroscopically ductile penetrative fabrics. In the field, ductile penetrative strain is most readily observed in pebbly sandstones and fine conglomerates with high proportions of weak lithic clasts (e.g. tuffs and mudstone). In these rocks, ductile deformation is localized in steeply dipping, NW-striking (Fig. 3a) high-strain zones ranging from meters to tens of meters wide. These zones generally become thicker and more common toward the contact with the Khaz Mélange. The high-strain zones have strongly linear fabrics, defined by aligned elongate pebbles, but generally lack well-developed planar cleavage fabrics. The pebbles typically have prolate shapes with aspect ratios between 4:1.5:1 and 5:2:1 (long axis:intermediate axis:short axis), but achieve ratios as high as 7:2:1. Average long axes of the pebbles from various sites trend E–W to NW–SE, and most plunge between 5° and 20° (Fig. 3b). Outside of the high-strain zones, pebbles usually have aspect ratios of 2:1 or less, and are rarely prolate-shaped. The linear fabrics are much less obvious in medium- to coarse-grained lithic arenite and graywacke that have more uniform grain sizes. The ductile high-strain zones occur across at least 3 km of the Sitka Graywacke southwest of the Khaz Mélange (note sample localities on Fig. 2), but do not constitute a single, homogenous high strain zone—rather, the high-strain zones seem to bound relatively undeformed blocks or slivers. However, because exposures are essentially limited to two-dimensional views along the coastline, the actual geometry and distribution of the high-strain zones at the map

scale is not clear. A poorly developed spaced cleavage cross-cuts the ductile fabrics within the high-strain zones, as well as bedding preserved outside of the high-strain zones, and thus appears to be related to deformation after formation of the high-strain zones. This observation is important because it indicates that the Sitka Graywacke was not penetratively deformed before formation of the high-strain zones. The cleavage generally strikes northwest and has steep southwest dips (Fig. 3d). Several sets of widely spaced joints are found throughout the Sitka Graywacke. Thin, well-defined cataclastic faults cross-cut the linear fabrics of the high-strain zones and are clearly related to later brittle deformation. The penetrative high-strain zones do not have distinct boundaries as is typical of the cataclastic faults.

### *Microscopic deformation*

Thin sections of the Sitka Graywacke reveal a variety of deformation mechanisms which acted during penetrative deformation of indurated lithic arenite and graywacke. Most of the macroscopically ductile penetrative strain occurred as dependent particulate flow in which space problems associated with particles moving past each other (i.e. the dilation requirement) are overcome by intragranular deformation (Borradaile, 1981; Bernabe and Brace, 1990). In the Sitka Graywacke, the intragranular deformation was accommodated primarily by grain-scale pressure solution and deformation of low-strength fine-grained lithic particles which were squeezed around and in between the higher strength particles (Fig. 4a). Some cataclasis of high-strength particles is evident as fractures and spalling. Although small in volume, fibrous quartz and white mica–chlorite beards on some particles document fluid-enhanced diffusive mass transfer related to pressure solution. Significant solid-state diffusion does not seem likely because the rocks lack textural evidence of crystal plastic deformation. Evidence for intergranular movement associated with dependent particle flow comes mostly from observations of offset fractured grains. Asymmetrically wrapped bearded overgrowths on some grains leads us to infer that particle rolling occurred during dependent particle flow, but evidence for particle rolling is uncommon. The pervasive nature of the micro-scale deformation suggests low pore fluid pressures during deformation (Bernabe and Brace, 1990; Wong, 1990).

Intragranular crystal plastic deformation textures, such as undulatory extinction, core–mantle structures, and embayed grain boundaries (Fig. 4b), are observed in many particles in the Sitka Graywacke, but are mostly inherited from the source rocks. Rotation recrystallization and grain boundary migration textures are best developed in polycrystalline quartz grains in which they are clearly cross-cut or truncated by abrasion surfaces developed during erosion and trans-

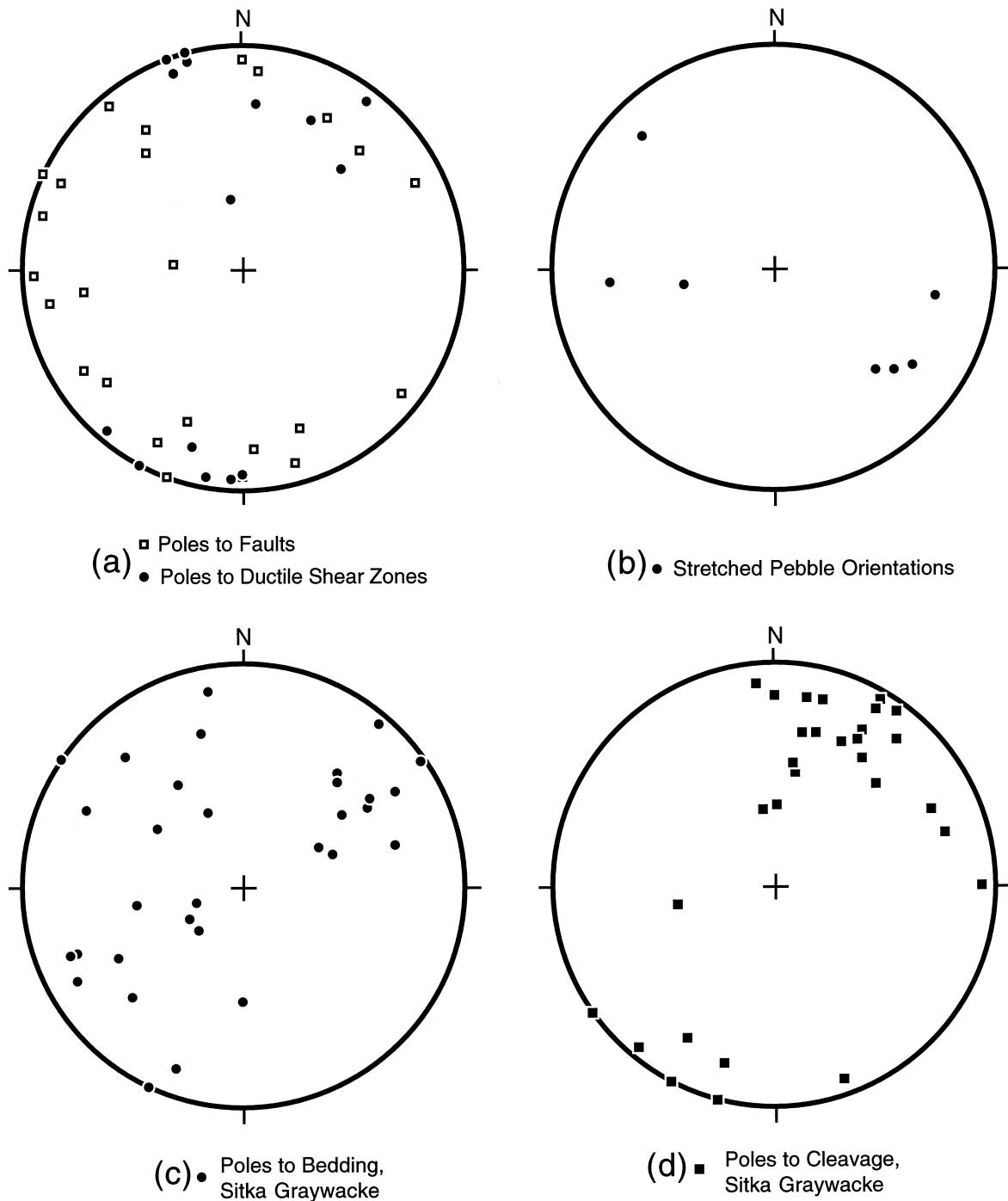


Fig. 3. Lower hemisphere equal area plots of (a) poles to brittle faults and ductile shear zones, (b) average orientation of long axes of stretched pebbles at various stations, (c) poles to bedding, and (d) poles to cleavage. All data measured from outcrops of the Sitka Graywacke located in the area of Fig. 2.

port (Fig. 4b), and thus, are textures inherited from the source area. Monocrystalline quartz grains with undulatory extinction are more problematic, and evidence for whether this texture was inherited from a source area or developed during penetrative deformation of the Sitka Graywacke is equivocal. We did not observe optically any tilt walls or subgrain formation in any of the quartz grains with undulatory extinction, which indicates only limited dislocation glide in the low temperature Regime 1 of Hirth and

Tullis (1992). Because dislocation glide leading to undulatory extinction in quartz can occur at temperatures typical of lowest greenschist facies or lower (Hirth and Tullis, 1992), development of the undulatory extinction during dependent particulate flow in the Sitka Graywacke cannot be ruled out as another intragranular deformation mechanism.

We infer that the penetrative deformation in the Sitka Graywacke must have occurred near the brittle-ductile transition in the accretionary complex.

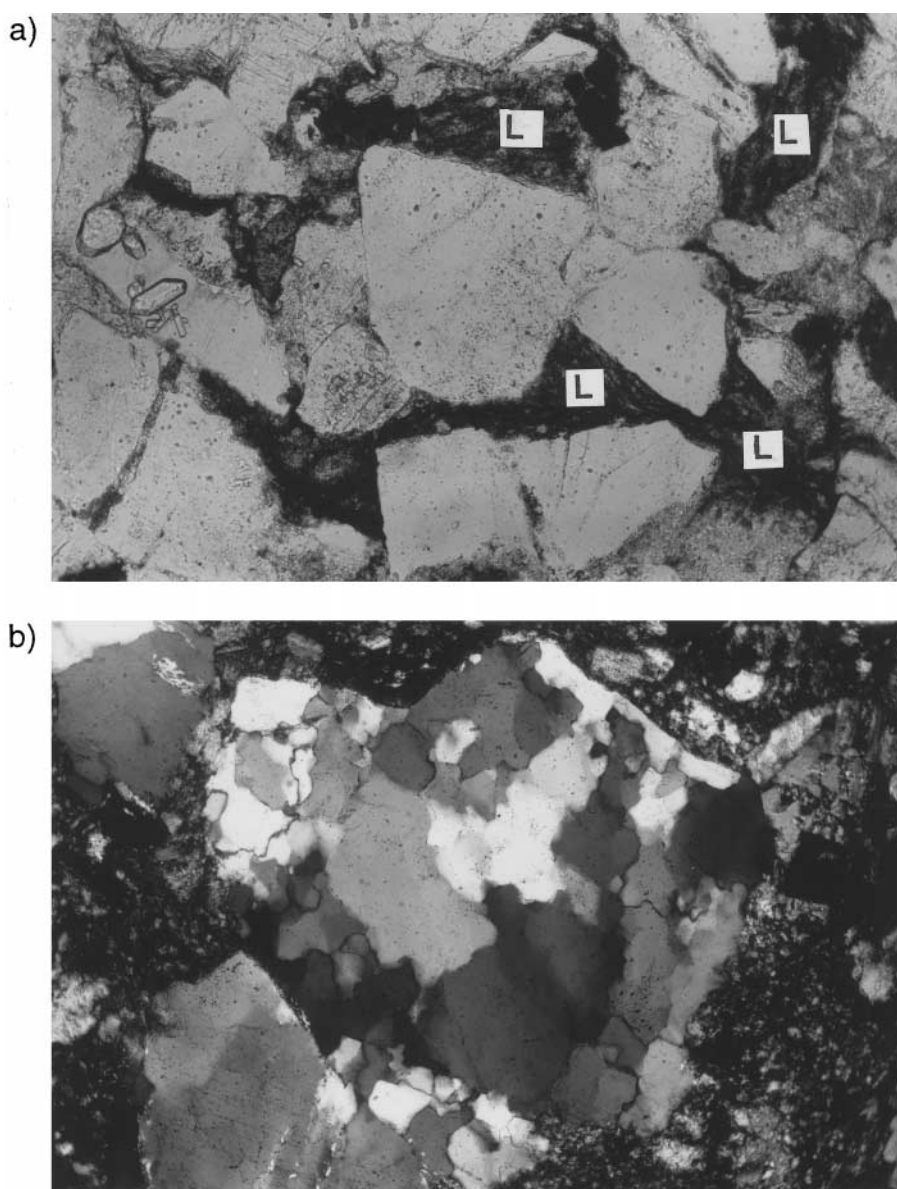


Fig. 4. Photomicrographs of the Sitka Graywacke showing (a) highly deformed lithic particles (L) that accommodated intergranular movements of competent grains (primarily quartz in this photograph). Plane polarized light; field of view  $1.7 \times 1.2$  mm; (b) clast having well developed crystal plasticity textures that are truncated at the grain boundaries. Crossed polarized light; field of view  $2.3 \times 1.8$  mm.

Evidence for deformation near the brittle–ductile transition primarily comes from the presence of diffuse penetrative high-strain zones, the lack of related thin, sharply defined cataclastic shear zones, the relatively limited amount of cataclastically deformed particles, and the ductilely deformed low-strength lithic clasts. Undulatory extinction in quartz could also indicate penetrative deformation near the brittle–ductile transition, but as pointed out above, may be a feature inherited from the source rocks.

#### *Kinematics of deformation in the high-strain zones*

In order to place the results of a finite strain analysis into a useful tectonic framework, the kinematics of the deformation leading to the finite strain must be

known. Without kinematic information, any number of deformation paths can yield a given finite strain. The kinematics of the high-strain zones in the Sitka Graywacke are difficult to establish because kinematic indicators are poorly developed. Field evidence includes porphyroclasts and a stretching lineation (115/10) in a lense of mylonitic marble near S93SIT-05 and rotated tension gashes in a variety of locations. These field kinematic indicators all yield dextral sense of shear. Microscopic kinematic indicators in the high-strain zones are lacking, or give ambiguous results. However, dextral kinematic indicators are well developed in samples S93SIT-05 and S93SIT-13, and include fractured and offset grains (microfaults at high angles to weakly formed shear bands are antithetic and those at low angles to subparallel to shear bands

are synthetic (e.g. Simpson, 1986)), quartz porphyroclasts with asymmetric tails ( $\sigma$  and  $\delta$ ), offset calcite veins, and microfolds in weak lithic fragments at diametrically opposite corners of competent clasts (cf. Simpson and Schmid, 1983). In addition to kinematic analysis of the Sitka Graywacke, we also analyzed retrograde ductile shear zones in the adjacent Khaz M elange. These ductile shear zones overprint the m elange fabric and are cross-cut by the brittle fault system that also cross-cuts the high-strain zones of the adjacent Sitka Graywacke. The ductile shear zones in the m elange increase in abundance toward the contact with the Sitka Graywacke; thus we infer that they formed at the same time as the high-strain zones, and the kinematics of these shear zones may be used to corroborate the kinematic information from the Sitka Graywacke. *S-C* fabrics and rotated porphyroclasts from the Khaz M elange mostly yield dextral kinematics, although in a few cases, sinistral kinematics are found. Thus, the available data most strongly indicate dextral kinematics for the high-strain zones in the Sitka Graywacke.

### STRAIN ANALYSIS

For this study, we obtained the general shape and orientation of finite-strain ellipsoids from seven localities (Fig. 2) in order to better understand the tectonic and deformational settings responsible for the high-strain zones and associated stretched conglomerates we observed in the Sitka Graywacke.

#### *Method*

For this study of the Sitka Graywacke we chose not to estimate finite strain using particle shape analyses (e.g.  $R_f/\phi_f$  method) because strong ductility contrasts between the strain markers (pebbles) and their matrix (sand or siltstone) can yield unreliable results (Freeman and Lisle, 1987; Paterson and Yu, 1994). Thus, in order to estimate the finite-strain ellipsoid of the high-strain zones we used the center-to-center grain separation technique first proposed by Ramsay (1967), and later modified by Fry (1979) and Erslev (1988).

In as much as the Sitka Graywacke is not perfectly sorted or packed, we obtained the two-dimensional finite strain data by using the Normalized Fry method (Erslev, 1988) which enhances the definition of the finite-strain ellipse of the resulting plot over that of the Fry method (Fry, 1979). The Normalized Fry method does not correct specifically for poor packing of particles in an aggregate, but it does result in better definition of the finite-strain ellipse. Several requirements must be satisfied before undertaking a Normalized Fry analysis. The undeformed rock must have a uniform (i.e. anticlustered) particle center distribution in three

dimensions, predeformation particle shapes should have low ellipticities, particle shape alteration by grain boundary migration or rotation recrystallization must be minimal in order to avoid mislocating the original grain centers, and the particles should have been packed (although not necessarily close packed) in the predeformation state to yield the best results. The Sitka Graywacke meets these various criteria fairly well with the exception of the last one. Although the Sitka Graywacke may have been packed in the undeformed state, the primary deformation mechanism, as discussed above, included extreme deformation of weak lithic clasts which were part of the original packed aggregate. Thus some of the particle centers chosen for the analysis of the deformed Sitka Graywacke may represent grains not originally in contact with each other, a factor that would introduce an element of scatter into the final plot and reduce the quality of definition of the finite strain ellipse. Overall, then, the sandstones of the Sitka Graywacke do not completely meet the criteria for successful application of a center-to-center strain analysis, but are nonetheless adequate to yield well defined strain ellipses.

We performed Normalized Fry analyses on oriented samples by cutting three mutually orthogonal ( $90^\circ \pm 2^\circ$ ) oriented thin sections from each sample and making photomicrographs of the thin sections. The photomicrographs were scanned and imported into a computer program ( $R_f/\text{Fry}$  5.1 by Earth'nWare for Macintosh computers) that approximates the shapes of chosen grains by manually fitted ellipses, calculates the grain centers, and performs the Normalized Fry analysis. Eighty  $\pm$  10 grain centers were used for each thin section, which yielded ellipses on resulting plots that were well enough defined to unambiguously choose a manual best fit ellipse (Fig. 5). In order to minimize possible grain center mislocations, we chose areas of the thin sections in which a majority of the grains were quartz, feldspar, amphibole and pyroxene that showed little or no evidence of ductile deformation, but which also contained a sufficient quantity of deformed lithic fragments to have accommodated dependent particulate flow. To assess repeatability of the results, multiple Normalized Fry analyses were performed on several of the samples. The results of the repeated analyses showed that both the shape and orientation of the ellipse were repeatable to within 10% variation. As discussed above, the use of only competent grains may introduce some scatter in the final plots since not all of these particles were necessarily in contact with each other originally. The two-dimensional ellipse data were compiled into three-dimensional strain ellipsoids following the orthographic method of De Paor (1986, 1990) and using his 2D-3D and Solve 3 Stretches programs.



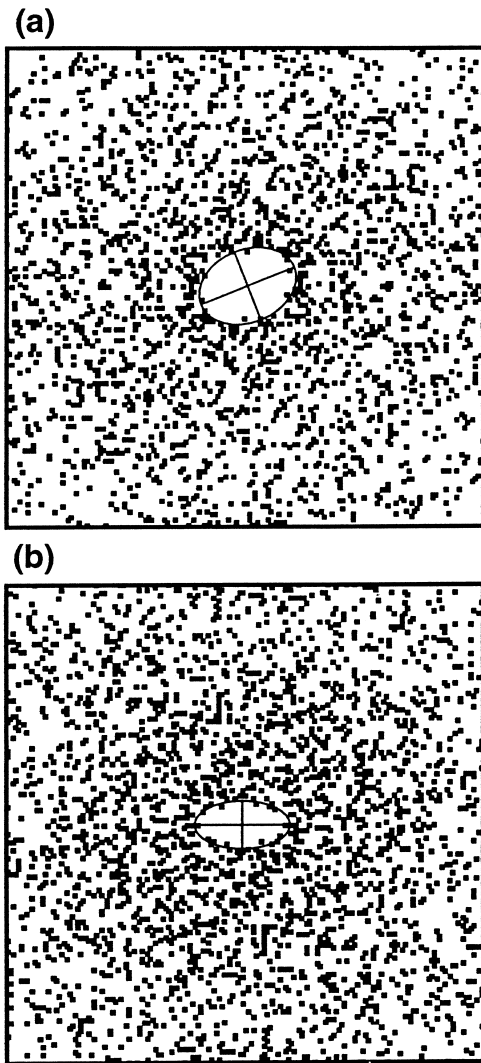


Fig. 5. Representative normalized Fry plots. (a) Sample S93SIT-13;  $R_s = 1.4$ ,  $\phi = 24^\circ$ , (b) Sample S93SIT-05;  $R_s = 2.2$ ,  $\phi = 0^\circ$ .

*Strain analysis results*

When the resulting finite-strain ellipsoids are plotted on a Flinn diagram (Fig. 6), five of seven fall in the apparent constrictional field with  $k$  ranging from 1.8 to 7, one plots in the apparent flattening field with  $k = 0.3$ , and one falls on the plane strain line with  $k = 1$ . The results are summarized in Table 1, from which it can be seen that the magnitudes of the apparent stretches ( $X =$  maximum principle stretch,  $Y =$  intermediate principle stretch,  $Z =$  minimum principal stretch) are relatively small. Orientations of the finite-strain ellipsoids vary somewhat, but the maximum principal stretches of the constrictional finite-strain ellipsoids generally trend SE–NW with shallow plunges (Fig. 7) and the maximum principal stretches of the strain ellipsoids lying in the plane strain and apparent flattening strain fields trend SW and NE, respectively (Fig. 8) and have shallow plunges. The minimum principal stretches of the plane and flattening finite-strain ellipsoids trend approximately N and S, respectively, and both plunge  $73^\circ$ .

Because the Sitka Graywacke lacks clasts of predictable size or proportion (such as fossils, oolites, etc.), volumetric strains cannot be directly estimated. Weakly, and sometimes moderately, developed pressure solution surfaces at both the grain and thin-section scales indicate some negative volumetric strains. The pressure solution surfaces are most easily visible in thin sections cut at high angles to the strike of the shear zones. In these sections, the pressure solution surfaces exhibit a variety of orientations, suggesting that volume loss was not preferentially developed in one direction as might be expected from sedimentary compaction or tectonically induced volume losses such as those modeled for transpressive shear zones by Dias and Ribeiro (1994). Textural evidence for positive volumetric strains includes fibrous chlorite and quartz overgrowths on grain surfaces oriented normal to pressure solution surfaces. The textural evidence for positive volumetric strains is relatively rare in comparison to evidence for negative volumetric strains. This suggests that the positive and negative volumetric strains either balance each other, or more likely, that the volumetric strains are probably negative and small, but without a preferred orientation. If the position of the plane strain line is recalculated for the Flinn diagram assuming various negative volumetric strains (10%, 20%), the plane strain sample (S93SIT-16) falls in the apparent constriction field, but all other samples remain in their original fields. Thus, the constrictional finite-strain ellipsoids probably record true constrictional strain that is not dependent on volumetric strain.

The orientations of  $X$  in the samples that yield constrictional finite-strain ellipsoids are similar to the orientations of a variety of penetrative lineations observed in the field (Fig. 7). These include a subhorizontal, SE-trending mylonite lineation near the contact of the Khaz Mélange and the Sitka Graywacke, mineral lineations in the Khaz Mélange, and strained pebble orientations measured in the Sitka Graywacke. The finite strain analysis also shows that the degree to which the

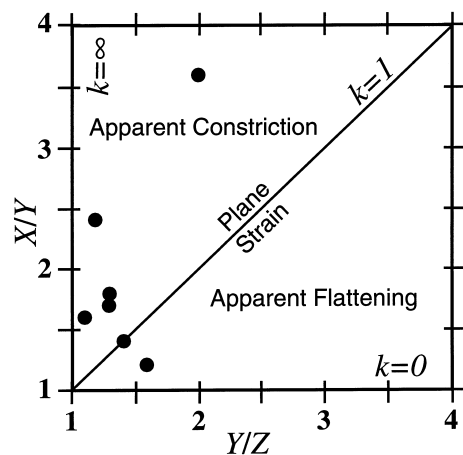


Fig. 6. Flinn diagram of the strain ellipsoid data presented in Table 1.

Table 1. Data from the strain analysis

Sample	<i>X</i>	<i>Y</i>	<i>Z</i>	<i>k</i> *	<i>X</i> Trend/Plunge	<i>Y</i> Trend/Plunge	<i>Z</i> Trend/Plunge
S93SIT-05	1.5	0.9	0.7	2.3	132/04	042/02	211/88
S93SIT-13	1.9	0.8	0.7	7.0	136/14	032/50	238/39
S93SIT-33	1.6	0.9	0.7	2.7	086/27	182/14	298/62
S93SIT-39	1.4	0.9	0.8	6.0	128/12	223/22	018/67
S93SIT-41	2.9	0.8	0.4	2.6	292/44	061/33	170/26
S93SIT-16	1.4	1.0	0.7	1.0	258/12	165/17	004/72
S93SIT-31	1.3	1.1	0.7	0.3	063/02	334/16	176/73

finite strains are constrictional is inhomogenous across the Sitka Graywacke. There is no clear correlation of the magnitude of strain or the degree to which it is constrictional with distance from the contact with the Khaz Mélange. Our calculated axial ratios of the constrictional finite-strain ellipsoids from the sandstones are somewhat less than the axial ratios measured from the conglomerate clasts in the field (see above), in general agreement with modeling by Freeman and Lisle (1987) which predicted that, where there are large competence contrasts between pebbles (high competence) and matrix (low competence), the pebble shapes will be markedly more prolate than the bulk strain ellipsoid measured from the matrix material. It is also possible that the higher axial ratios of the conglomerate clasts may relate to locally higher strains or an initial clast ellipticity upon which a constrictional finite strain was superimposed.

## DISCUSSION OF RESULTS

### Constrictional strains

Most scenarios for developing constrictional strains rely on one of two mechanisms: interference between

sequentially imposed, non-coaxial plane or flattening strains (e.g. Marty, 1994; Marty and Pavlis, 1994; Pavlis and Sisson, 1995) or viscous/plastic flow of magma or rock in a shear zone having a non-tabular shape such as a diapir (e.g. Toriumi and Noda, 1986; Orange, 1990; John and Blundy, 1993). Another setting for constrictional finite strains was documented by Fletcher and Bartley (1994) who showed that such strains form in low-angle extensional shear zones in metamorphic core complexes by shortening parallel to the shear zone and normal to the transport direction. Numerical modeling by Dias and Ribeiro (1994) showed that constrictional strains can form in transpressive shear zones if lateral escape of material from the ends of the shear zones is coupled with large negative volumetric strain. The volumetric strain may result in vertical shortening (in the case of transpression superimposed on a diagenetic volume loss) or horizontal shortening (tectonically induced volume loss related to transpression), although horizontal shortening must also be coupled to a vertical shear across the ends of the shear zones.

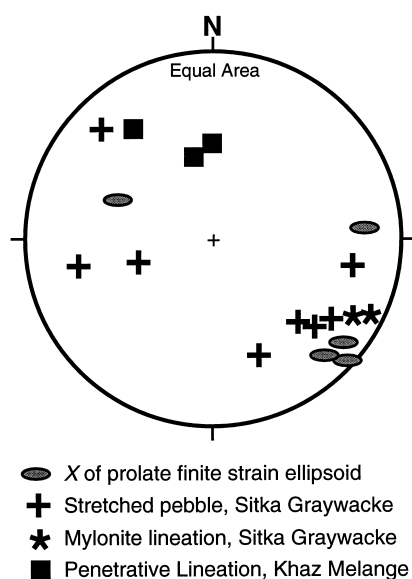


Fig. 7. Lower hemisphere equal area plot of *X* principal stretch orientations of the constrictional strain ellipsoids, and penetrative lineations measured in the Sitka Graywacke and the Khaz Mélange in the area of Fig. 2.

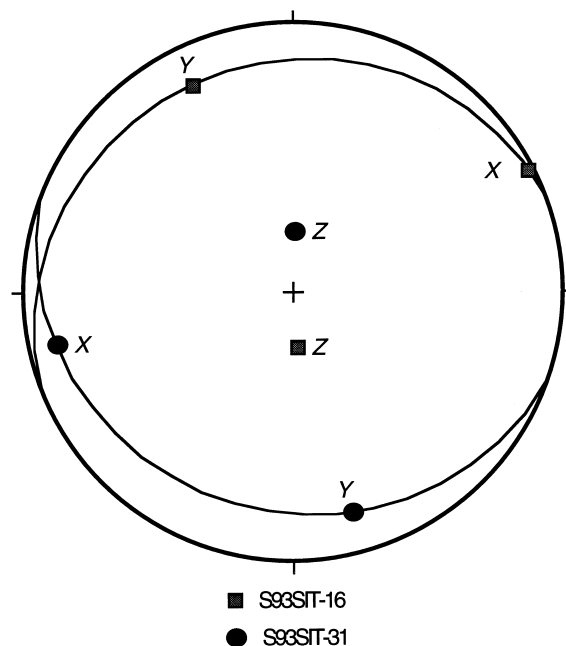


Fig. 8. Lower hemisphere equal area plot of the principal stretch (*X*, *Y*, *Z*) orientations and *X*/*Y* principal plane of the plane ( $k = 1$ ) and flattening ( $k < 1$ ) strain ellipsoids. The plane strain ellipsoid is represented by squares and the flattening strain ellipsoid is represented by dots.

Where sequentially imposed non-coaxial flattening strains have been called upon to explain constrictional strains, there is usually good macroscopic evidence, such as multiple cleavages. However, evidence for sequential development of non-coaxial flattening strains is absent in the Sitka Graywacke. The cleavage consists of a weakly developed spaced cleavage that is difficult to observe in outcrop and only has one orientation. The cleavage clearly formed after the ductile high-strain zones formed, and there is no evidence of a penetrative deformation prior to formation of the ductile high-strain zones. That leads us to consider that the constrictional strains which formed in the ductile high-strain zones developed during penetrative ductile flow of the clastic rocks, as discussed above.

Diapiric intrusions in accretionary complexes have elliptical to round cross sections and steeply plunging  $X$  axes of constrictional finite-strain ellipsoids (Orange, 1990), and thus do not correspond to the data and observations from the Sitka Graywacke. Instead, the tabular geometry of the ductile high-strain zones and shallow plunges of  $X$  axes of the constrictional finite-strain ellipsoids most likely represent zones of general shear. Furthermore, the orientations of the high-strain zones and their  $X$  axes correspond approximately with the orientations of ductile shear zones and penetrative lineations observed in the Khaz Mélange near the contact with the Sitka Graywacke. These considerations lead us to interpret the penetrative, ductile, high-strain zones in the Sitka Graywacke as ductile shear zones which have dextral kinematics (see above discussion).

#### *Plane and flattening strains*

The deformation leading to the plane and flattening finite-strain ellipsoids of samples S93SIT-16 and S93SIT-31 is difficult to attribute to any of the common deformational processes for sediments or sedimentary rocks. In both samples, the  $X$ - $Y$  principal plane strikes between  $50^\circ$  and  $60^\circ$  differently and dips between  $25^\circ$  and  $40^\circ$  shallower than bedding planes at the outcrops from which the samples were taken. Likewise, nearly all cleavage orientations in the Sitka Graywacke dip  $>50^\circ$  more steeply than the  $X$ - $Y$  principal plane, and at the outcrops from which the samples were taken, the cleavage also has markedly different strikes (compare Figs 3d & 8). Thus, these finite-strain ellipsoid shapes probably did not result from shortening normal to layering during sediment consolidation, nor from cleavage formation during folding. Thus we are uncertain of the significance of the plane and flattening strain ellipsoids, and they may be the result of noise or error in the strain analysis and of little structural significance.

#### *Implications of constrictional strains in the Sitka Graywacke*

The dextral ductile shear zones in the Sitka Graywacke must have kinematics that are able to produce a constrictional finite strain. Dextral simple shear zones or those with shortening across them produce plane or flattening finite strains (Sanderson and Marchini, 1984; Fossen and Tikoff, 1993) and cannot produce a constrictional finite strain without lateral extrusion of material coupled with substantial volume loss and additional shearing in specific orientations (Dias and Ribeiro, 1994). Well-developed cleavage parallel to the shear zone boundary is predicted for all cases of transpression. Because we cannot directly document the volumetric strain, or its orientation, it is difficult to evaluate whether or not the transpressive volume loss model of Dias and Ribeiro (1994) applies to the Sitka Graywacke. However, as discussed above, the evidence for volume loss such as pressure solution surfaces is generally weakly developed or entirely absent in the dextral shear zones of the Sitka Graywacke. Where pressure solution surfaces are developed in the dextral shear zones, they are developed subparallel to the long axes of the shear zones, but have a wide variety of orientations with respect to the shear zone boundaries and lack a preferred orientation. Thus it seems unlikely, but not impossible, that the results of our strain analysis can be explained by volume loss in a dextral transpressive shear zone.

Fletcher and Bartley (1994) discuss a model for the occurrence of fold axes parallel to the stretching lineations in ductile shear zones of low-angle normal faults. They infer that the lineation-parallel fold axes grow during ductile shearing by shortening of the shear zone parallel to the shear zone boundaries, but perpendicular to the stretching lineation. If one applies the low-angle extension fault model of Fletcher and Bartley (1994), but turns their shear zone on edge, it is possible to reproduce the constrictional finite strain and kinematics of the dextral ductile shear zones in the Sitka Graywacke. The result is a shear zone in which there is vertical shortening parallel to  $Y$ , and if volume is conserved, either extension parallel to the shear zone or, in the case discussed by Fletcher and Bartley (1994), extension across the shear zone (i.e. at a high angle to the shear zone boundaries) in order to make room for the generation of folds with movement-parallel axes. For strike-parallel stretching of a ductile shear zone, strain compatibility with surrounding rock requires similar stretching of the surrounding rocks. Since the dextral ductile shear zones of this study are of limited thickness, and surrounding rocks do not show evidence of penetrative ductile strain or coeval brittle failure, this kinematic scenario is unlikely. Therefore, we are left to consider that the constrictional finite strains formed in ductile shear zones that have a component of extension across them. As dis-

cussed above, the kinematics of these ductile shear zones is dominantly dextral. This combined with the easterly plunge of four of the  $S_1$  axes of the constrictional ellipsoids in NE dipping to vertical shear zones requires that the latter are dextral transtensional shear zones (Sanderson and Marchini, 1984; Fossen and Tikoff, 1993).

A transtensional ductile shear zone and related constrictional finite strains can result from homogenous deformation related to superposition of extension across a simple shear zone. If volume is conserved, the resulting divergence of the shear zone boundaries requires material flow parallel to the shear zone boundaries and towards its center which would result in crustal thinning, a situation seemingly unlikely in the relatively narrow confines of a shear zone. However, in the brittle part of the crust, the extension could be accommodated by normal faulting distributed over a larger area than that affected by the ductile transtensional shear zones. Alternatively, if strains are constrictional and volume is conserved, the shear zone may become shorter with increasing strain, a geologically unreasonable circumstance. Another possibility is that the constrictional finite strain formed as the result of convergent flow around a kilometer-scale asperity within a thick shear zone. This is almost impossible to evaluate in ancient settings, especially in relatively narrow shear zones as it would be fortuitous if we sampled each of them at local asperities. Thus, we infer that the constrictional strains formed during homogenous transtensional deformation within ductile shear zones and that volume was conserved through local crustal thinning.

The orientation of the  $X$  axes of the constrictional finite-strain ellipsoids determined in this study is not wholly consistent with transtensional shear zones. Modeling by Fossen and Tikoff (1993) and Fossen *et al.* (1994) shows that the  $X$  orientation of the finite-strain ellipsoid in a transtensional shear zone should trend obliquely to the shear zone boundaries, whereas in the Sitka Graywacke  $X$  is subparallel to the strike of the shear zone boundaries (compare Fig. 3a with Fig. 7). Because of the essentially two-dimensional view of the ductile shear zones that we obtained in the field, we do not know the true orientation of the major shear zones in the area. Most of the shear zones represented in Fig. 3(a) are relatively thin (< 2 m) and appear to anastomose around blocks of less deformed material, so that while their orientations parallel the  $X$  axes, they are not directly related to the thicker shear zones from which the constrictional finite strains were recorded. In addition, although there is some evidence in support of a transpressional origin for the constrictional strains ( $X$  is subparallel to the measured shear zone boundaries, Fossen *et al.*, 1994), the textural evidence (no or very weak shear zone cleavage, minor volume loss, volume loss in a wide variety of orien-

tations) most strongly suggests a transtensional origin for the constrictional strains (Fossen *et al.*, 1994).

#### *Tectonic significance of transtension in the Sitka Graywacke*

In light of the foregoing discussion, two types of tectonic models may be invoked to explain constrictional finite strains that formed in the Sitka Graywacke in a subduction zone setting: (1) contemporaneous superposition (or interference) of two plane or flattening strains related to shearing against both the downgoing slab and backstop formed by the overriding plate (e.g. Fig. 9; Toriumi and Noda, 1986), or (2) a local transtensional environment within the subduction complex (Fig. 10), which is our preferred type of model.

Contemporaneous superposition of two plane or flattening strains in a subduction zone is possible and is consistent with the kinematics of oblique convergence along the western margin of North America for the Late Cretaceous (Engebretson *et al.*, 1985). In this type of model, the contemporaneous interference or superposition of two flattening or plane finite strains occurs through shearing of the prism of material caught between an obliquely subducting slab and the backstop of the overriding plate. This results in constriction and lateral flow (stretching) of that material (Fig. 9; Toriumi and Noda, 1986). Applying such a model to the Sitka Graywacke requires simultaneous oblique shearing against the Khaz M elange, which would act as the non-deforming backstop, and subducting plate (which would act as the non-deforming lower plate). The Sitka Graywacke caught in the triangular prism formed by the bounding plates would then flow parallel to the intersection of the two plates, resulting in constrictional strains. Although the Khaz M elange probably was deformed during the ductile shear zone event, as evidenced by the retrograde shear zones discussed above, if the strain rate of the Khaz M elange was less than the strain rate of the Sitka Graywacke then the former would approximate a non-deforming backstop. This scenario is possible, but difficult to evaluate.

The second type of tectonic scenario, that of a transtensional environment in a subduction zone setting, is our preferred option (Fig. 10). Initially, transtension in a subduction zone may seem contradictory to generally accepted models, but it is entirely possible if convergence is oblique and partitioned into dip-slip and strike-slip components. Superposition of contemporaneous trench-normal extension on the partitioned dextral strike-slip component could result in dextral transtension. Possible mechanisms for trench-normal extension in a convergent setting include gravity driven wedge-taper adjustment (Davis *et al.*, 1983; Platt, 1986) related to overthickening of the 'hinterland' portion of an accretionary wedge, changes in the normal component of relative plate motions, or subduction of

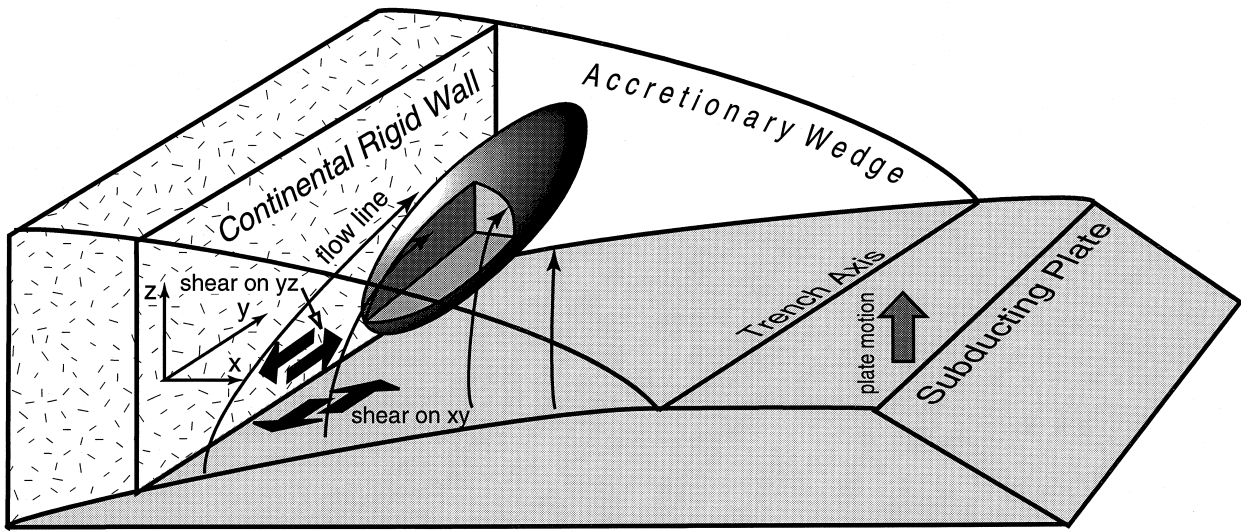


Fig. 9. Sketch showing model proposed by Toriumi and Noda (1986) with constrictional finite-strain ellipsoid added. Modified after Toriumi and Noda (1986).

a topographic asperity, such as an oceanic spreading ridge (e.g. Berhman *et al.*, 1994). Operation of any of these mechanisms during oblique convergence could produce an element of extension across an oblique transcurrent ductile shear zone at depth and produce transtension. Such oblique transtensional shear zones would yield shallowly plunging constrictional finite strain ellipsoids within them. The transtension may accommodate only a portion of the extensional strain; the rest may be accommodated by normal faults.

The Late Mesozoic to Early Cenozoic tectonics of the western margin of North America provide the appropriate setting in which to develop transtension by simultaneous plate motion partitioning and trench-normal extension. During this period, all of the mech-

anisms for trench normal extension could have operated, but it is most likely that trench-normal extension resulted from an underplating event. The Chugach accretionary complex formed during the Late Cretaceous to Middle Eocene along an oblique convergent margin (Engebretson *et al.*, 1985) in which partitioning of the oblique convergence would have resulted in the formation of dextral strike-slip shear zones in the forearc (Sitka Graywacke). Trench-normal extension during the Eocene subduction of the Kula-Farallon spreading ridge under North America (Marshak and Karig, 1977; Engebretson *et al.*, 1985; Bradley *et al.*, 1993; Sisson and Pavlis, 1993), in a manner similar to the subduction of the Chile Rise under southern South America (Behrmann *et al.*,

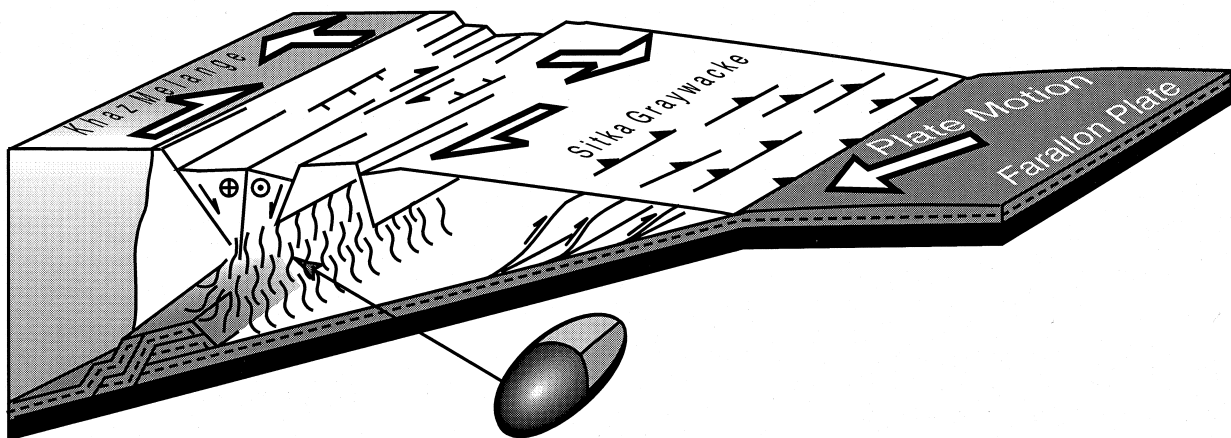


Fig. 10. Schematic representation of the formation of a transtensional shear zone in the Sitka Graywacke. Sediment underplating (thrust duplex in lower left) and overthickening of the Sitka Graywacke induced trench normal extension which was superimposed on a dextral strike-slip shear zone activity partitioning the strike-slip component of oblique plate convergence. This superposition of extension on the dextral ductile shear zone resulted in dextral transtension and formation of constrictional finite strains in the ductile shear zone (note the location and orientation of the prolate finite-strain ellipsoid). Extension in the brittle upper part of the Sitka Graywacke occurred on normal faults.

1994), could have produced transtension if superimposed on dextral shear zones. Alternatively, the subducting ridge could have acted as a local asperity causing vertical shortening in the Chugach accretionary complex, which, when superposed on the dextral shear zones, also could produce constrictional strains. However, in the Chugach accretionary complex, brittle deformation contemporaneous with subduction of the Kula–Farallon ridge is manifested as conjugate strike-slip faults related to shortening normal to the trench (Bradley and Kusky, 1990, 1992; Bradley *et al.*, 1993). Our field work clearly shows that the conjugate brittle faults crosscut the ductile transtensional shear zones of this study (c.f. Haeussler *et al.*, 1994). Thus, we conclude that ridge subduction post-dates and is unrelated to formation of the transtensional ductile shear zones in the Sitka Graywacke.

Because ridge subduction, and the deformation associated with it, post-dated formation of the transtensional shear zones, we conclude that the trench-normal extension must relate to wedge taper adjustments related to underplating or plate motion changes that occurred prior to Eocene ridge subduction beneath the southern Chugach accretionary complex. A rough calculation of the angle of convergence between the Farallon and North America plates, based on plate motion vectors of Engebretson (1985) and Lonsdale (1988) and the orientation of the North America margin proposed by Pavlis and Sisson (1995), shows that convergence was markedly more oblique before the 56 Ma–52 Ma plate reorganization than after. Therefore, it is unlikely that a change in convergence obliquity related to passage of the Kula–Farallon spreading ridge was responsible for trench-normal extension in the Chugach accretionary complex.

In view of the preceding discussion we propose that the transtensional nature of the dextral strike-slip shear zones in the Sitka Graywacke resulted from the contemporaneous superposition of underplating and overthickening-driven wedge taper adjustments on dextral strike-slip shear zones which were actively partitioning the Late Cretaceous–Eocene oblique plate convergence. Late Cretaceous–Early Paleocene underplating and thickening of the Chugach accretionary wedge is documented for the Kodiak Formation on Kodiak Island (Sample and Moore, 1987). The Kodiak Formation is likely to be an along-strike equivalent of the Sitka Graywacke, and if Tertiary strike-slip separations are restored, then the Sitka Graywacke may well have undergone the same underplating event. Therefore, the Sitka Graywacke could have experienced simultaneous dextral shearing and trench-normal extension with the resultant formation of dextral transtensional shear zones. Although this model is speculative, we believe it best fits our strain analyses, field observations, regional geology and existing plate kinematic models.

## CONCLUSION

The Sitka Graywacke of the Chugach accretionary complex contains dextral ductile shear zones which have constrictional finite strains, a surprising find in the inherently compressional tectonic environment represented by a forearc. Several tectonic models may be invoked to explain the constrictional strains in the dextral shear zones of the Sitka Graywacke. Among these, dextral transpression is attractive because an accretionary complex is generally a compressional environment. However, other than the orientations of the  $X$  principal axes in the constrictional finite-strain ellipsoids, no evidence can be forwarded to support transpression, and textural evidence argues against it. A likely origin for the constrictional finite strain observed in the ductile shear zones of the Sitka Graywacke is dextral transtension in an oblique convergent subduction zone setting. Such a model requires both partitioning of oblique plate convergence and contemporaneous trench-normal extension of the forearc. Although the orientation of the  $X$  principal axes of the constrictional finite strain ellipsoids from the ductile shear zones in the Sitka Graywacke is not fully consistent with transtension, textural evidence supports transtension. The presence of dextral transtensive shear zones in the Late Cretaceous–Early Cenozoic forearc of SE Alaska is broadly consistent with strain (kinematic) partitioning of oblique convergence between North America and the downgoing Farallon plate. Transtension in the dextral ductile shear zones may have resulted from contemporaneous superposition of an accretionary wedge-taper adjustment, related to an underplating event, subduction of a topographic asperity such as a spreading ridge, or a change in relative plate motions. Our preferred option is superposition of strike-slip partitioning of oblique plate convergence with trench-normal extension of the Chugach accretionary complex during the Late Cretaceous–Paleocene underplating event documented elsewhere in the Chugach accretionary complex. Further studies along strike are needed in order to determine if the constrictional strains and dextral shear zones were a response to a localized tectonic event, or if they represent a significant regional tectonic event.

*Acknowledgements*—This paper represents a portion of JSD's doctoral dissertation research. Financial support for JSD was provided by a John T. Dillon Alaska Research Award from the Geological Society of America, and by the Volunteer Program of the U.S. Geological Survey, Alaska Branch. Rick Allmendinger's Stereonet Program was used to generate the stereonet plots. Early versions of this manuscript were greatly improved by numerous constructive comments from Don Fisher, Peter Haeussler, Terry Pavlis, David Scholl, Basil Tikoff, and Robert Twiss. We thank JSG reviewers Jinny Sisson and Jim Hibbard for numerous thoughtful comments on this version of the manuscript. We also thank Associate Editor Richard Norris.

## REFERENCES

- Avé Lallemant, H. G. and Guth, L. R. (1990) Role of extensional tectonics in exhumation of eclogites and blueschists in an oblique subduction setting, Northeastern Venezuela. *Geology* **18**, 950–953.
- Behrmann, J. H., Lewis, S. D. and Cande, S. C. (1994) ODP Leg 141 Scientific Party, Tectonics and geology of spreading ridge subduction at the Chile Triple Junction: a synthesis of results from Leg 141 of the Ocean Drilling Program. *Geologisches Rundschau* **83**, 832–852.
- Berg, H. C., Jones, D. L. and Richter, D. H. (1972) Gravina–Nutzotin belt; Tectonic significance of an upper Mesozoic sedimentary and volcanic sequence in southern and southeastern Alaska. *U.S. Geological Survey Professional Paper* **800-D**, D1–D24.
- Bernabe, Y. and Brace, W. F. (1990) Deformation and fracture of Berea Sandstone. In *The Brittle–Ductile Transition in Rocks, The Heard Volume*, ed. A. G. Duba, W. B. Durham, J. W. Handin and H. F. Wang. Geophysical Monograph, **56**, pp. 91–101. American Geophysical Union.
- Borradaile, G. J. (1981) Particulate flow of rock and the formation of cleavage. *Tectonophysics* **72**, 305–321.
- Bradley, D. C., Haeussler, P. J. and Kusky, T. M. (1993) Timing of early Tertiary ridge subduction in southern Alaska. In *Geologic Studies in Alaska by the U.S. Geological Survey, 1992*, ed. C. Dusel-Bacon and A. B. Till. Geological Survey Bulletin **2068**, pp. 163–173.
- Bradley, D. C. and Kusky, T. M. (1990) Kinematics of late faults along Turnagain Arm, Mesozoic accretionary complex, south-central Alaska. In *Geologic Studies in Alaska by the U.S. Geological Survey, 1989*, ed. J. K. Dover and J. P. Galloway. U.S. Geological Survey Bulletin **1946**, pp. 3–10.
- Bradley, D. C. and Kusky, T. M. (1992) Deformation history of the McHugh Complex, Seldovia quadrangle, south-central Alaska. In *Geologic studies in Alaska by the U.S. Geological Survey, 1990*, ed. D. C. Bradley and A. Ford. U.S. Geological Survey Bulletin **1999**, pp. 17–32.
- Cashman, S. M., Kelsey, H. M., Erdman, C. F., Cutten, H. N. C. and Berryman, K. R. (1992) Strain partitioning between structural domains in the forearc of the Hikurangi subduction zone, New Zealand. *Tectonics* **11**, 242–257.
- Cloos, M. and Shreve, R. L. (1988) Subduction channel model of prism accretion, mélange formation, sediment subduction, and subduction erosion at convergent plate margins: 2. *Pure and Applied Geophysics* **128**, 501–545.
- Cowan, D. S. (1994) Alternative hypothesis for the mid-Cretaceous paleogeography of the western Cordillera. *GSA Today* **4**, 181–186.
- Davis, D., Suppe, J. and Dahlen, F. A. (1983) Mechanics of fold-and-thrust belts and accretionary wedges. *Journal of Geophysical Research* **88(B2)**, 1153–1172.
- De Paor, D. G. (1990) Determination of the strain ellipsoid from sectional data. *Journal of Structural Geology* **12**, 131–137.
- De Paor, D. G. (1986) Orthographic analysis of geological structures—II. Practical applications. *Journal of Structural Geology* **8**, 87–100.
- Decker, J. and Johnson, B. R. (1981) The nature and position of the Border Ranges fault on Chichagof Island. In *The U. S. Geological Survey in Alaska: Accomplishments During 1979*, ed. N. R. D. Albert and R. Hudson. U.S. Geological Survey Circular **823-B**, pp. B102–B104.
- Decker, J., Nilsen, T. H. and Karl, S. (1979) Turbidite facies of the Sitka Graywacke, southeastern Alaska. In *The U. S. Geological Survey in Alaska: Accomplishments During 1978*, ed. K. M. Johnson and J. R. William. U.S. Geological Survey Circular **804-B**, pp. B125–B129.
- Dias, R. and Ribeiro, A. (1994) Constriction in a transpressive regime: an example in the Iberian branch of the Ibero–Armorican arc. *Journal of Structural Geology* **16**, 1543–1554.
- Engelbreton, D. C., Cox, A. and Gordon, R. G. (1985) Relative motions between oceanic and continental plates in the Pacific Basin. *Geological Society of America Special Paper* **206**.
- Erslev, E. A. (1988) Normalized center-to-center strain analysis of packed aggregates. *Journal of Structural Geology* **10**, 201–209.
- Fitch, T. J. (1972) Plate convergence, transcurrent faults, and internal deformation adjacent to southeast Asia and the western Pacific. *Journal of Geophysical Research* **77**, 4432–4460.
- Fletcher, J. M. and Bartley, J. M. (1994) Constrictional strain in a non-coaxial shear zone: Implications for fold and rock fabric development, central Mojave metamorphic core complex, California. *Journal of Structural Geology* **16**, 555–570.
- Fossen, H. and Tikoff, B. (1993) The deformation matrix for simultaneous simple shearing and volume change, and its application to transpression–transtension tectonics. *Journal of Structural Geology* **15**, 413–422.
- Fossen, H., Tikoff, B. and Teyssier, C. (1994) Strain modeling of transpressional and transtensional deformation. *Norsk Geologisk Tidsskrift* **74**, 134–145.
- Freeman, B. and Lisle, R. J. (1987) The relationship between tectonic strain and the three-dimensional shape fabrics of pebbles in deformed conglomerates. *Journal of the Geological Society of London* **144**, 635–639.
- Fry, N. (1979) Random point distributions and strain measurement in rocks. *Tectonophysics* **60**, 89–105.
- Haeussler, P. J., Davis, J. S., Roeske, S. M. and Karl, S. M. (1994) Late Mesozoic and Cenozoic faulting history at the leading edge of North America, Chichagof and Baranof Islands, southeastern Alaska. *Geological Society of America Abstracts with Programs* **26**, A–317.
- Hirth, G. and Tullis, J. (1992) Dislocation creep regimes in quartz aggregates. *Journal of Structural Geology* **14**, 145–159.
- Jarrard, R. D. (1986) Relations among subduction parameters. *Reviews of Geophysics* **24**, 217–284.
- John, B. E. and Blundy, J. D. (1993) Emplacement-related deformation of granitoid magmas, southern Adamello Massif, Italy. *Geological Society of America Bulletin* **105**, 1517–1541.
- Johnson, B. R. and Karl, S. M. (1985) Geologic map of western Chichagof and Yakobi Islands, southeastern Alaska. *U.S. Geological Survey Misc. Invest. Map* **I-1506**, scale 1:125,000.
- Karig, D. E., Lawrence, M. B., Moore, G. F. and Curray, J. R. (1980) Structural framework of the fore-arc basin, NW Sumatra. *Journal of the Geological Society of London* **137**, 77–91.
- Karig, D. E., Sarewitz, D. R. and Haeck, G. D. (1986) Role of strike-slip faulting in the evolution of allochthonous terranes in the Philippines. *Geology* **14**, 852–855.
- Karl, S. M., Brew, D. A. and Wardlaw, B. R. (1990) Significance of Triassic marble from Nakwasina Sound, southeastern Alaska. In *Geologic Studies in Alaska by the U. S. Geological Survey, 1989*, ed. J. H. Dover and J. P. Galloway. Geological Survey Bulletin **1946**, pp. 21–28.
- Kelsey, H. M., Cashman, S. M., Beanland, S. and Berryman, K. R. (1995) Structural evolution along the inner forearc of the obliquely convergent Hikurangi margin, New Zealand. *Tectonics* **14**, 1–18.
- Loney, R. A., Brew, D. A., Muffler, L. J. P. and Pomeroy, J. S. (1975) Reconnaissance geology of Chichagof, Baranof, and Kruzof Islands, southeastern Alaska. *U.S. Geological Survey Professional Paper* **792**.
- Lonsdale, P. (1988) Paleogene history of the Kula plate: Offshore evidence and onshore implications. *Geological Society of America Bulletin* **100**, 733–754.
- Marshak, S. R. and Karig, D. E. (1977) Triple junctions as a cause for anomalously near-trench igneous activity between the trench and volcanic arc. *Geology* **5**, 233–236.
- Marty, K. (1994) Finite strain analysis of the Chugach Accretionary Complex: Implications for tectonic processes, Richardson Highway Transect, Alaska. M.S. thesis, University of New Orleans.
- Marty, K. and Pavlis, T. (1994) Finite strain analysis of the Chugach Accretionary Complex along the Richardson Highway, southern Alaska: Evidence for transpression following subduction accretion. *Geological Society of America Abstracts with Programs* **26(7)**, A–73.
- McCaffrey, R. (1991) Slip vectors and stretching of the Sumatran forearc. *Geology* **19**, 881–884.
- Monger, J. W. H., Price, R. A. and Tempelman-Kluit, D. J. (1982) Tectonic accretion and the origin of the two metamorphic and plutonic belts in the Canadian Cordillera. *Geology* **10**, 70–75.
- Monger, J. W. H. and Price, R. A. (1996) Comment on “Paleomagnetism of the Upper Cretaceous strata of Mount Tatlow: Evidence for 3000 km of northward displacement of the eastern Coast Belt, British Columbia” by P. J. Wynne *et al.*, and on “Paleomagnetism of the Spences Bridge Group and northward displacement of the Intermontane Belt, British Columbia: A sec-

- ond look" by E. Irving *et al.*, *Journal of Geophysical Research*, **101**, pp. 13793–13799.
- Monger, J. W. H., van der Heyden, P., Journeay, J. M., Evenchick, C. A. and Mahoney, J. B. (1994) Jurassic–Cretaceous basins along the Canadian Coast Belt: their bearing on pre-mid-Cretaceous sinistral displacement. *Geology* **22**, 175–178.
- Orange, D. L. (1990) Criteria helpful in recognizing shear-zone and diapiric mélanges: Examples from the Hoh accretionary complex, Olympic Peninsula, Washington. *Geological Society of America Bulletin* **102**, 935–951.
- Paterson, S. R. and Yu, H. (1994) Primary fabric ellipsoids in sandstones: implications for depositional processes and strain analysis. *Journal of Structural Geology* **16**, 505–517.
- Pavlis, T. L. and Sisson, V. B. (1995) Structural history of the Chugach metamorphic complex in the Tana River region, eastern Alaska: A record of Eocene ridge subduction. *Geological Society of America Bulletin* **107**, 1333–1355.
- Plafker, G., Jones, D. L. and Pessagno, E. A. Jr (1977) A Cretaceous accretionary flysch and mélange terrane along the Gulf of Alaska margin. In *The U.S. Geological Survey in Alaska: Accomplishments During 1976*, ed. K. M. Blean. U.S. Geological Survey Circular **751-B**, pp. B41–B43.
- Plafker, G., Jones, D. L., Hudson, T. and Berg, H. C. (1976) The Border Ranges fault system in the Saint Elias Mountains and Alexander Archipelago. In *The U.S. Geological Survey in Alaska: Accomplishments During 1975*, ed. E. H. Cobb. U.S. Geological Survey Circular **733**, pp. 14–16.
- Plafker, G., Moore, J. C. and Winkler, G. R. (1994) Geology of the southern Alaska margin. In *The Geology of Alaska*, ed. G. Plafker and H. C. Berg, G-1, pp. 389–449. Geological Society of America, Boulder, Colorado.
- Platt, J. P. (1986) Dynamics of orogenic wedges and the uplift of high-pressure metamorphic rocks. *Geological Society of America Bulletin* **97**, 1037–1053.
- Ramsay, J. G. (1967) *Folding and fracturing of rocks*. McGraw-Hill Book Company, New York.
- Reed, J. C. and Coats, R. R. (1941) Geology and ore deposits of the Chichagof mining district, Alaska. *U.S. Geological Survey Bulletin* **929**.
- Rubin, C. M., Saleeby, J. B., Cowan, D. S., Brandon, M. T. and McGroder, M. F. (1990) Regionally extensive mid-Cretaceous west-vergent thrust system in the northwestern Cordillera: implications for continent-margin tectonism. *Geology* **18**, 276–280.
- Sample, J. C. and Moore, J. C. (1987) Structural style and kinematics of an underplated slate belt, Kodiak and adjacent islands, Alaska. *Geological Society of America Bulletin* **99**, 7–20.
- Sanderson, D. J. and Marchini, W. R. D. (1984) Transpression. *Journal of Structural Geology* **6**, 449–458.
- Sisson, V. B. and Pavlis, T. L. (1993) Geologic consequences of plate reorganization: An example from the Eocene southern Alaska fore arc. *Geology* **21**, 913–916.
- Simpson, C. (1986) Determination of movement sense in mylonites. *Journal of Geological Education* **34**, 246–261.
- Simpson, C. and Schmid, S. (1983) An evaluation of criteria to deduce the sense of movement in sheared rocks. *Geological Society of America Bulletin* **94**, 1281–1288.
- Toriumi, M. and Noda, H. (1986) The origin of strain patterns resulting from contemporaneous deformation and metamorphism in the Sambagawa metamorphic belt. *Journal of Metamorphic Geology* **4**, 409–420.
- Walcott, R. I. (1987) Geodetic strain and the deformational history of the North Island of New Zealand during the late Cainozoic. *Philosophical Transactions of the Royal Society of London* **A321**, 163–181.
- Wong, T-F. 1990. Mechanical compaction and the brittle–ductile transition in porous sandstones. In *Deformation Mechanisms, Rheology, and Tectonics*, ed. R. J. Knipe and E. H. Rutter. Geological Society Special Publication **54**, pp. 111–122.
- Wynne, P. J., Irving, E. J., Maxson, A. and Kleinspehn, K. L. (1995) Paleomagnetism of the Upper Cretaceous strata of Mount Tatlow: Evidence for 3000 km of northward displacement of the eastern Coast Belt, British Columbia. *Journal of Geophysical Research* **100**, 6073–6091.
- Wynne, P. J., Thorkelson, D. J., Kleinspehn, K. L., Maxson, J. A. and Irving, E. (1996) Paleomagnetism of the Upper Cretaceous strata of Mount Tatlow: Evidence for 3000 km of northward displacement of the eastern Coast Belt, British Columbia. Reply. *Journal of Geophysical Research* **101**, 13801–13803.